ChemPubSoc Europe

DOI: 10.1002/chem.201902981

CHEMISTRY A European Journal Full Paper

Hybrid Materials

A Low-Temperature Approach for the Phase-Pure Synthesis of MIL-140 Structured Metal–Organic Frameworks

Marcel Schulz, Nele Marquardt, Malte Schäfer, Dawid Peter Warwas, Saskia Zailskas, and Andreas Schaate*[a]

Abstract: In a systematic investigation, the synthesis of metal–organic frameworks (MOFs) with MIL-140 structure was studied. The precursors of this family of MOFs are the same as for the formation of the well-known UiO-type MOFs although the synthesis temperature for MIL-140 is significantly higher. This study is focused on the formation of Zr-based MIL-140 MOFs with terephthalic acid (H_2*bdc*), biphenyl-4,4′-dicarboxylic acid (H_2*bpdc*), and 4,4′-stilbenedicarboxylic acid (H_2*sdc*) and the introduction of synthesis field diagrams to discover parameters for phase-pure products. In this context, a MIL-140 network with H_2*sdc* as linker molecule is first reported. Additionally, an important aspect is the reduction of the synthesis temperature to make MIL-140 MOFs more accessible even though linkers with a more delicate nature are used. The solvothermal syntheses were conducted in highly concentrated reaction mixtures whereby a targeted synthesis to yield the MIL-140 phase is possible. Furthermore, the effect of the often-used modulator approach is examined for these systems. Finally, the characteristics of the synthesized MOFs are compared with physisorption measurements, thermogravimetric analyses, and scanning electron microscopy.

Introduction

In the last few decades, metal–organic frameworks (MOFs) have received growing attention from researchers. Formed by inorganic building units (IBUs) and organic linker molecules, MOFs belong to the family of porous coordination polymers.[1] Their properties can be widely controlled by using different metal cations and organic linkers for their construction. MOFs often exhibit a high surface area and, with increasing length of the linker molecule, the pore size is tunable.[2] The pore interior can be modified by using linker molecules with different functionalities.[3,4] Owing to this modular composition, tailored materials for applications such as gas storage and separation,[5] drug delivery systems,[6] catalysts,[7] or as sensing materials[8] are possible.

An outstanding representative of this group of materials is the zirconium-based MOF UiO-66 (UiO: universitetet i oslo), which was firstly described by the Lillerud group.[9] In contrast to other frameworks, based on zinc or copper, Zr-based MOFs exhibit exceptional chemical and thermal stabilities.[10,11] With the synthesis of UiO-66, Cavka et al. presented a three-dimensional framework in which the IBUs are twelvefold connected by terephthalates, forming an extended *fcu* framework. This and the high oxidation state of the Zr^{4+}, resulting in a high Zr–O bonding energy, are the main reasons for the high stability of these frameworks. With an elongation of the linker molecules, the isoreticular series of UiO-67 (H_2*bpdc*: biphenyl-4,4′-dicarboxylic acid) and UiO-68 (H_2tpdc) was reported. To obtain crystalline materials, it is beneficial to add further additives to the synthesis of UiO-67 or UiO-68. In the so-called modulation approach, monocarboxylic acids are added to the reaction mixture to slow down the nucleation of the MOF. Owing to the competition reaction between the modulator and the linker for the Zr^{4+} cations, the reversibility of the formation is increased, which leads to more ordered materials and larger crystals.[12]

The pore sizes and the surface areas increase from UiO-66 to UiO-68. A disadvantage of the frameworks with longer linker molecules is the decreasing stability.[11] Indeed, UiO-67 shows the same thermal stability as UiO-66 but decomposes in the presence of water.[13]

With the increasing popularity of the UiO frameworks, a large number of linkers have been used to obtain functionalized materials with UiO structure.[14] Thus, the uptake of certain gases can be enhanced and allows the use of functionalized UiO-66 frameworks as sensor materials.[15] Either with the direct synthesis of functionalized materials or post-synthetic modification,[4,16] by which other substituents can be introduced, a decreased pore size and surface area follows. For this

[a] M. Schulz, N. Marquardt, M. Schäfer, D. P. Warwas, S. Zailskas, Dr. A. Schaate
Institute of Inorganic Chemistry and ZFM—Center for Solid State Chemistry and New Materials, Leibniz University Hannover
Callinstr. 9, 30167 Hannover (Germany)
E-mail: andreas.schaate@acb.uni-hannover.de

Supporting information and the ORCID identification number(s) for the author(s) of this article can be found under: https://doi.org/10.1002/chem.201902981.

reason, the accessibility of these groups can be limited as well as the usability, for example, in a sensing device.

By using the same linker molecules, Guillerm et al. presented new Zr-based MOFs with even higher chemical and thermal stability.[17] In contrast to the UiO materials, the so-called MIL-140 series exhibits chains of sevenfold coordinated Zr cations as IBUs, which are oriented parallel to the *c*-axis of the structure. Each zirconium oxide chain is connected to six other chains, resulting in a three-dimensional framework. The corresponding tube-like one-dimensional pore system is located in the voids between three Zr-oxide chains (see Figure 1). Owing

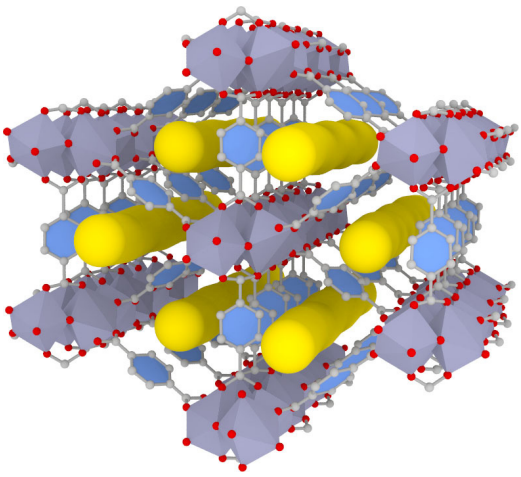

Figure 1. Representation of the surrounding of one zirconium oxide chain in MIL-140A, which is connected via terephthalates to six other chains. The resulting one-dimensional tube-like pore system (yellow) is indicated by yellow spheres (dark blue polyhedra: Zr; red: oxygen; gray: carbon).

to this one-dimensionality, the Brunauer–Emmett–Teller (BET) surfaces and the pore sizes of these materials are slightly lower than the materials with *fcu* topology. The MIL-140 series is characterized by a higher thermal stability than the UiO series (ca. 500 vs. ca. 450 °C) and exhibits a higher stability concerning mechanical pressure. In contrast to UiO materials, the members of the MIL-140 series are stable in boiling water.[17] This higher tolerance towards water can be explained with the more hydrophobic character of the MOFs. In case of the MIL-140B, an interesting potential application is the protection of cultural heritage through a high adsorption of acetic acid from air without degradation.[18]

To date, there are only a few groups focusing on the synthesis of MIL-140 MOFs or computational studies.[18–21] According to Guillerm et al., for the successful synthesis of MIL-140, high temperatures are needed, otherwise the UiO phase is obtained. For this reason, they estimated that the UiO-66 phase represents the kinetic product whereas the MIL-140A phase is the thermodynamic one. The group of D'Allesandro focused on microwave-assisted synthesis of MIL-140 frameworks. They were able to yield a variety of different functionalized MIL-140A frameworks with a very short reaction time, which were impossible to synthesize by using conventional heating.[21,22] In a recently published investigation, Butova et al. were able to control the synthesis of the system UiO/MIL-140 with addition of water.[23] The authors of the study argued that upon addition of water to the synthesis mixture, Zr oxide nanoparticles are formed, which lead to the selective crystallization of UiO-66. In that work, the synthesis temperature of 220 °C is still as high as in the original work. Wang et al. used a different approach.[24] They conducted their MOF synthesis at 185 °C and ended up with a mixture of UiO-66 and MIL-140-A. The authors discuss that the differing surface charge of the two phases can be exploited to separate both from each other by adding negatively charged magnetic beads to the as-synthesized product mixture. In contrast to UiO-66, MIL-140A is negatively charged and shows no interaction with the beads. Consequently, only the UiO-66 particles are adsorbed onto the magnetic beads and can be separated from the product mixture.

Taking all this into account, we revisited the synthesis of frameworks with MIL-140 structure to examine the synthesis parameters, where a phase-pure material can be obtained. A very important aspect of this investigation is the reduction of the reaction temperature. With a reduced reaction temperature it will be possible to introduce thermally instable functional groups in the future, (e.g., azido-groups for sensing applications).[25] Additionally, the control on the resulting phase under more moderate conditions will make MIL-140-type frameworks more accessible because instead of high-pressure vessels, commonly used glass vials can be used for the synthesis.

The present work is focused on the synthesis of MIL-140A, C, and D. In contrast to the published MIL-140D, we used 4,4′-stilbenedicarboxylic acid (H_2*sdc*) instead of the azo-bridged linker molecule for the synthesis of a MIL-140D analog material. In consideration of that, we are able to use a commercially available linker and present a new framework with MIL-140 structure, the MIL-140D-*sdc*. For the first time, we present the successful syntheses of MIL-140 frameworks at 150 and 120 °C. Finally, we want to examine in a systematic study the crystallization behavior of the MIL-140 compounds and to establish synthesis field diagrams with areas of phase-pure products.

Results

We investigated systematically the synthesis of the three MOFs, MIL-140A, C, and D-*sdc*, and focused on a controlled synthesis to avoid the crystallization of the corresponding UiO phase. In our approach, we evaluated the formation of the MOFs through a defined choice of reaction parameters, like the precursor or modulator concentration as well as the reaction temperature and time. These fundamental studies are of great importance for the targeted synthesis of MIL-140 structured MOFs to avoid unwanted byproducts. As is known from the literature,[9] the use of terephthalic acid (H_2*bdc*) and $ZrCl_4$ in a solvothermal reaction in DMF leads to the formation of the prototypical Zr-MOF UiO-66. To obtain this MOF and other UiO-type materials, the typical ratio of metal salt and linear ditopic linker in the synthesis mixture is 1:1, which corresponds well with the sum formula of the final product (for UiO-66: $Zr_6O_4(OH)_4$(*bdc*)$_6$). In many published syntheses, the reaction mixtures are highly diluted because either the solubility of the

linker is low or the aim of the synthesis is the production of single crystals for structural determination. The corresponding ratio between metal salt and solvent ranges from 1:500 to 1:2000.[26] A typical synthesis temperature is 120 °C or lower in the case of functionalized linkers with delicate groups.[27] For the synthesis of MIL-140-type materials, several changes of the synthesis parameters are proposed. The synthesis of MIL-140A (ZrO(*bdc*)), for example, is conducted at a temperature of 220 °C and a ratio of $ZrCl_4$/H_2*bdc*/DMF of 1:2:80.[17] So, the synthesis mixture has a higher concentration compared with the synthesis of UiO-type materials and an excess of linker is used to obtain the phase-pure product. According to the authors, the high synthesis temperature is necessary to obtain the MIL-140 material because lower temperatures lead to the related UiO-type material. One of our aims in this study was the reduction of the synthesis temperature to prevent the necessity of autoclaves and thereby making the MIL-140-type materials more accessible. Thus, we reduced the synthesis temperature of our experiments to 150 °C or lower. For more detailed reaction parameters, see Tables S1–S12 in the Supporting Information.

Synthesis of MIL-140A

Influence of precursor concentration

We examined the influence of the precursor concentration on the outcome of MIL-140A syntheses by systematically varying the amount of DMF in the synthesis mixture. The ratio of H_2*bdc* and $ZrCl_4$ was kept at 1:1 whereas the amount of DMF was varied between 120 and 20 equivalents. The products obtained from syntheses at a temperature of 150 °C and a reaction time of 24 h show an evolution of the products from UiO-66 to MIL-140A depending on the amount of DMF. The PXRD patterns of both compounds show intensive diffraction peaks at similar positions but can be distinguished from each other easily: UiO-66 shows first peaks at $2\theta = 7.37$ and 8.52°, whereas the peaks of MIL-140A are at $2\theta = 7.45$ and 8.74° (see Figure S1 in the Supporting Information). Furthermore, the intensities of the two diffraction peaks are inverted for both materials.

According to the literature, no modulator is needed to obtain phase-pure MIL-140A.[17] By comparing the PXRD patterns of the corresponding products from syntheses conducted for 24 h without the addition of modulators (see Figure 2a), it can be seen that UiO-66 is formed when an amount of 120 or 100 equivalents of DMF are used. With 80 equivalents of DMF and below, the phase-pure synthesis of MIL-140A is possible. In a very concentrated synthesis mixture (20 equiv DMF) the diffraction peaks appear broader, indicating the formation of nanoparticles.

With the addition of 10 equivalents of acetic acid as a modulating agent, a different observation can be made (see Figure 2b). Considering the two reflections around $2\theta = 8.6$°, it is evident that in the range between 120 and 80 equivalents of DMF, a mixture of UiO-66 and MIL-140A is produced. Comparable to the results of the unmodulated synthesis, with high precursor concentrations (20 to 60 equiv DMF) only MIL-140A is

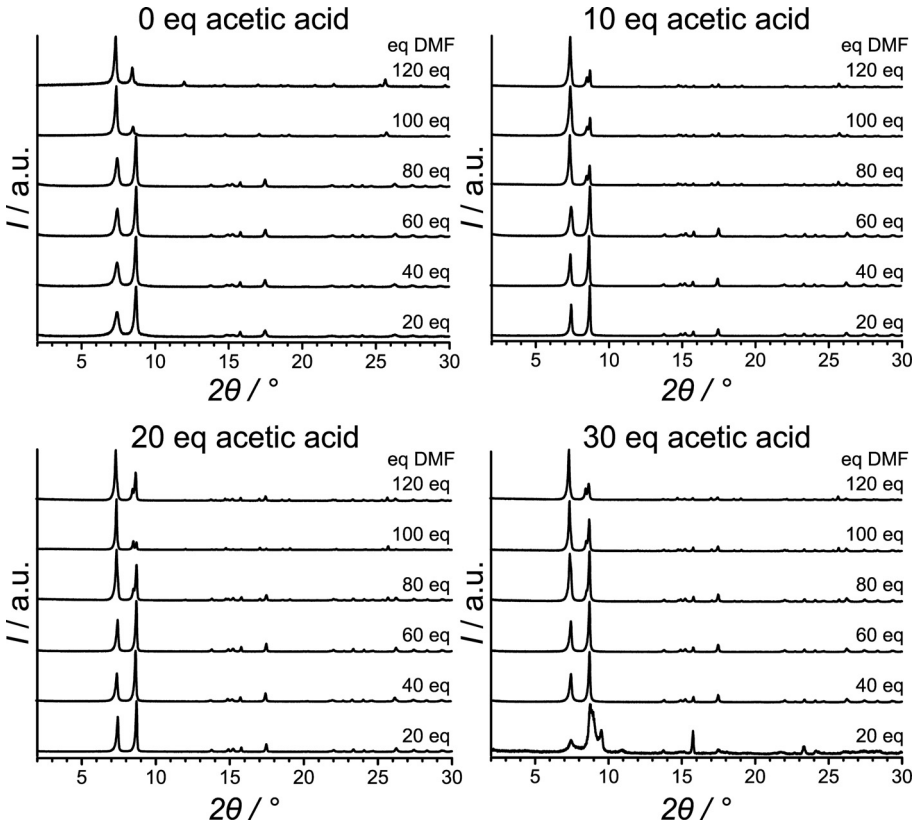

Figure 2. PXRD patterns of the products obtained from the systematic investigation of the formation of MIL-140A with different amounts of acetic acid. The PXRD patterns are arranged according to the amount of DMF from 20 to 120 equivalents.

obtained. By increasing the amount of acetic acid up to 20 and 30 equivalents, similar results can be obtained (Figure 2c and d). An exception is the synthesis with 20 equivalents DMF and 30 equivalents acetic acid, where additional diffraction peaks are observed and those of the MIL-140A appear broader. This experiment was repeated with a longer reaction time of 72 h ending up with a phase-pure MIL-140A (Figure 2). As a consequence, the diffraction pattern of the 24 h synthesis can be described as a pre-phase.

The summary of these results in a synthesis field diagram renders two distinct areas (Figure 3). Above approximately

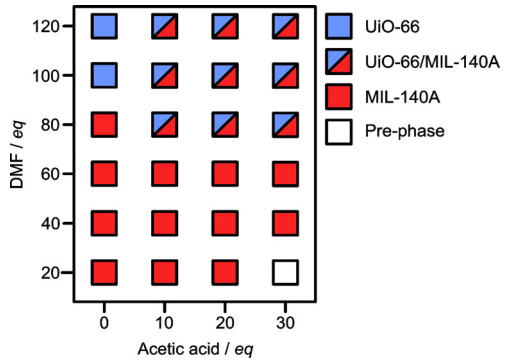

Figure 3. Synthesis field diagram of the UiO-66/MIL-140A system. The individual phases were assigned from PXRD for products from reactions for 24 h at 150 °C.

80 equivalents DMF lies an area where UiO-66 co-crystallizes with MIL-140A. Conducting the synthesis at a higher dilution with all other parameters kept constant yields only UiO-66. In this synthesis area and in even higher dilutions the formation of UiO-66 is usually described. It becomes clear that a phase-pure synthesis of MIL-140A is very feasible if the reaction is conducted in highly concentrated synthesis mixtures (60 equiv of DMF and less). Under these conditions, the linker (H_2bdc) is not completely dissolved. Either the presence of undissolved linker or the strongly acidic reaction conditions promote the formation of the MIL-140A phase. Naturally, the interaction of both can be necessary, too. It is conceivable that UiO-66 precipitates at first, followed by a degradation of this framework under acidic conditions and a recrystallization of MIL-140A. However, we found no evidence to support that theory. Instead, the product of the synthesis with the highest concentration of 20 equivalents of DMF and 30 equivalents of acetic acid yield a preliminary phase. After increasing the reaction time of this approach from 24 to 72 h, there is only MIL-140A present in the PXRD (Figure S2 in the Supporting Information).

After these first results of the UiO-66/MIL-140A system it is clear that the precursor concentration has a strong impact on the formed products. At the same time, the addition of a modulator affects the formation of the frameworks. The SEM investigation of the sample prepared with 60 equivalents of DMF and 30 equivalents of acetic acid reveals platelet-like particles, which are partly grown together (see Figure 4, left). In accordance with the crystallographic data (long *a*- and *b*-axis, short *c*-axis), the platelets show a short dimension perpendicular to

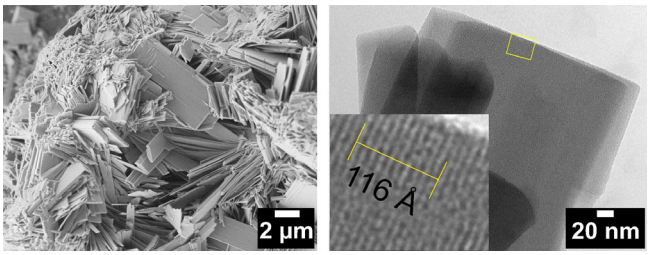

Figure 4. Left: SEM image of a MIL-140A sample obtained from a synthesis with 60 equivalents DMF and 30 equivalents acetic acid for 24 h at 150 °C with a magnification of 5000. Right: TEM image of the same sample. The distance between the two yellow lines indicates the distance between ten lattice planes.

the viewer, which make them appear very thin. For this reason, we used TEM for higher resolution. In the TEM images, lattice planes are visible and the average distance between the planes is about 11.6 Å (see Figure 4, right). A comparison with the cell parameters shows a length of the *b*-axis of 11.18 Å. With this good agreement, the lattice planes (0 *b* 0) are perpendicular to the observer. Including the other dimensions (long *a*- and short *c*-axis) and the very thin proportion of the crystal, we assume that the view of the crystal is along the *c*-axis.

Influence of reaction temperature

An important parameter for MOF syntheses is the reaction temperature. Under more moderate conditions, thermally unstable groups can be introduced to the framework and the material becomes more interesting for different applications. To investigate this issue, the parameters of a synthesis that yielded phase-pure MIL-140A (40 equiv DMF, 30 equiv acetic acid) were chosen as the starting point. The temperature of this synthesis was reduced from 150 °C to 120 °C whereas the synthesis time was extended from 24 h to 72 h. As shown in Figure 5, it is possible to obtain a crystalline material with parameters as described. A closer inspection reveals broadened diffraction peaks for the low-temperature synthesis but leaves no doubt of the purity of the MIL-140A phase. This could be an indication for the presence of nanoparticles. To prove that

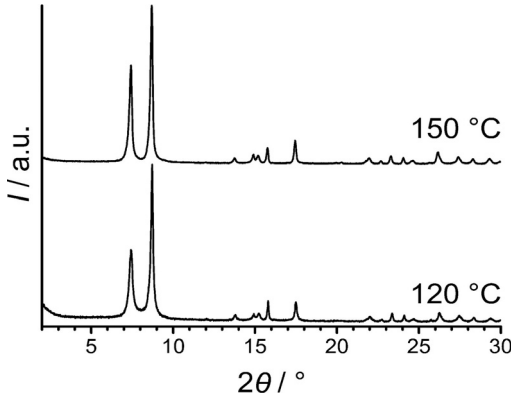

Figure 5. PXRD patterns of two MIL-140A products from syntheses with 40 equivalents DMF and 30 equivalents acetic acid for 72 h at 120 °C and for 24 h at 150 °C.

there are no amorphous impurities, we compared the products synthesized at 150 and 120 °C with Ar physisorption measurements (Figure S3 in the Supporting Information). Both compounds exhibit the same BET surface area of around 300 $m^2 g^{-1}$ (Table S13 in the Supporting Information).

Synthesis of MIL-140C

Influence of precursor concentration

As already discussed for the synthesis of MIL-140A, the precursor concentration has an influence on the precipitated material. In the following experiments, this behavior is investigated for the formation of MIL-140C. For this purpose, the same reaction parameters as for the UiO-66/MIL-140A system are chosen, with a reaction temperature of 150 °C and 24 h reaction time. The amount of DMF in the synthesis mixture was varied systematically between 20 and 120 equivalents and the ratio of H_2*bpdc* and $ZrCl_4$ was kept at 1:1. The amount of acetic acid was also varied between 0 and 30 equivalents. As for the UiO-66/MIL-140A system, the two compounds can be easily distinguished by their most intensive diffraction peaks. The first two reflections of MIL-140C ($2\theta = 5.56$ and 6.30°) occur at smaller diffraction angles than those of UiO-67 ($2\theta = 5.71$ and 6.59°) and the intensity ratios are reversed (Figure S4 in the Supporting Information).

With special attention to the PXRD patterns of the unmodulated syntheses, neither of the two phases precipitate. With an increased precursor concentration in the reaction mixture (20 equiv DMF), the broad reflection at $2\theta = 6.2°$ becomes more defined (see Figure 6a). This diffraction pattern could originate from an unknown phase of the MIL-140C, which is further described in the characterization section.

As already mentioned, the addition of a modulator is useful to synthesize UiO-67 or MIL-140C.[12,17,28] Upon the addition of acetic acid (10 to 30 equiv), crystalline products can be obtained (see Figure 6b–d). In general, there are three different areas discernible depending on the concentration of precursors in the synthesis mixture. Diluted precursor mixtures (100 equiv DMF and more) yield MIL-140C and UiO-67 as product mixtures. In the range between 60 and 80 equivalents DMF, the resulting phase depends on the modulator concentration. The purity of MIL-140C is increased when a higher amount of modulator is used. Similar results can be observed concerning the products of very concentrated reaction mixtures (20 and 40 equiv DMF). With an addition of only 10 equivalents of acetic acid, the MIL-140C phase is formed. With higher amounts of modulator, an additional phase precipitates until the modulator concentration is so high that the linker H_2*bpdc* is obtained.

In summary, there is an optimal range regarding the precursor concentration, which is shifted with an increasing amount of acetic acid to higher dilutions. This behavior is shown in the synthesis field diagram in Figure 7. In contrast to the systematic investigation for the UiO-66/MIL-140A system, in which it is possible to synthesize MIL-140A from highly concentrated synthesis mixtures, the synthesis of MIL-140C has more parameters to consider. First of all, a modulator is absolutely necessary to obtain a crystalline material under these conditions. Without

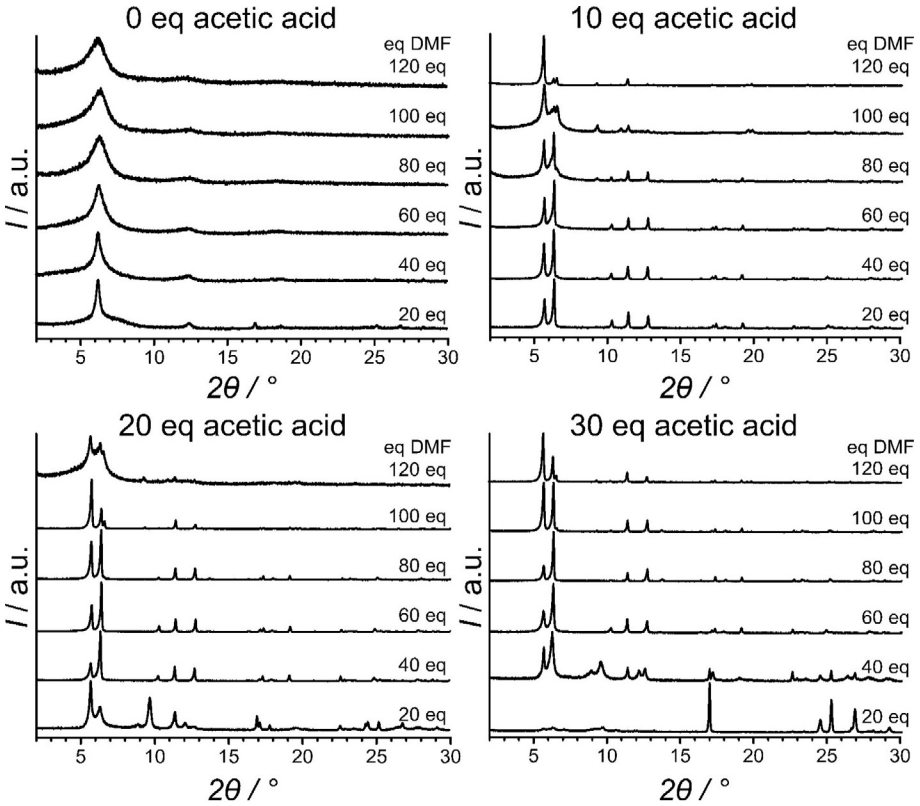

Figure 6. PXRD patterns of the products obtained from the systematic investigation of the formation of MIL-140C with different amounts of acetic acid. The PXRD patterns are arranged according to the amount of DMF from 20 to 120 equivalents.

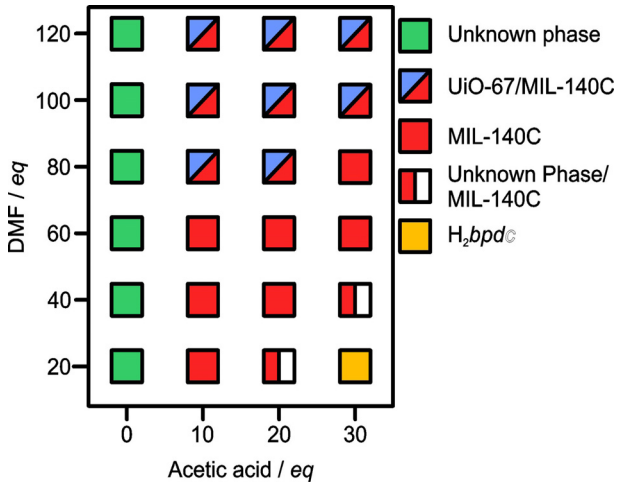

Figure 7. Synthesis field diagram of the UiO-67/MIL-140C system. The individual phases were assigned from PXRD for products from reactions for 24 h at 150 °C.

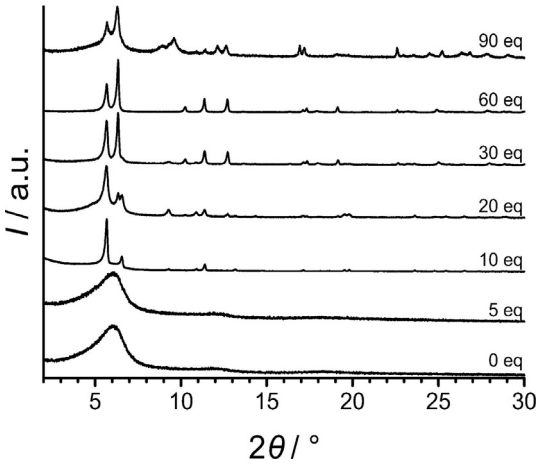

Figure 8. PXRD patterns of the products obtained from a synthesis with an increasing amount of acetic acid (bottom to top: 0, 5, 10, 20, 30, 60, and 90 equiv).

the addition of acetic acid, a structurally unknown phase is formed. Moreover, the change of the resulting phase mixture of UiO-67 and MIL-140C to pure MIL-140C is dependent on the precursor concentration, which can be seen in Figure 6. In contrast to MIL-140A, the ranges are shifted to slightly higher dilutions owing to the lower solubility of H_2*bpdc*. Consequently, with further addition of acetic acid, less linker can be dissolved in DMF and the phase-pure synthesis of MIL-140C is only possible with a higher DMF dilution. Nevertheless, the right concentration of the precursors is again a requirement for the successful preparation of phase-pure MIL-140 frameworks.

Influence of modulator concentration

As described above, the concentration of the precursors as well as the amount of modulator have an influence on the product formation of the UiO-67/MIL-140C system. In the next experiments, the amount of DMF was set to 130 equivalents and the ratio between H_2*bpdc* and $ZrCl_4$ remained unchanged. The reaction temperature was kept at 150 °C but the reaction time was increased to 72 h. To investigate the influence of the modulator on the product phases, the amount of acetic acid was varied between 0 and 90 equivalents.

As already mentioned, the use of modulating agents becomes very useful in Zr-MOF syntheses with longer linker molecules. This observation can also be made in these experiments (see Figure 8). Without the addition of acetic acid or with a too low amount (below 10 equiv), the synthesis yields an amorphous product or UiO-67. This is in good agreement with the crystallization behavior of UiO-67 reported in the literature or as mentioned before. A further increase in the amount of modulator results in the formation of a phase mixture of UiO-67 and MIL-140C. With an addition of 30 equivalents of acetic acid, UiO-67 is only a byproduct and by using 60 equivalents of acetic acid a phase-pure synthesis of MIL-140C is possible. When using higher concentrations of acetic acid, again a second phase can be noticed (compare with Figure 6d). Clearly, UiO-67 can only be synthesized in pure form with 10 equivalents acetic acid whereas higher amounts favor the formation of MIL-140C. This corresponds well with the crystallization behavior as is shown in the synthesis field diagram in Figure 7. The area of phase-pure MIL-140C synthesis is shifted to higher amounts of modulator and to higher dilutions.

The results of the PXRD patterns are further investigated with SEM investigation (Figure S5 in the Supporting Information). With an increasing amount of acetic acid from 10 to 60 equivalents at 130 equivalents DMF, the morphology changes from spherical particles to platelet-like particles.

Influence of reaction temperature and time

With these insights into the crystallization of MIL-140C, the reaction time and reaction temperature were varied. For these purposes, the experiment with 30 equivalents acetic acid and 80 equivalents DMF was chosen because the reaction produces phase-pure MIL-140C. With a reaction temperature of 150 °C, the reaction time was varied between 2 and 72 h. Even after only 2 h MIL-140C is formed, indicating a fast reaction rate. Nevertheless, the yield is significantly lower than after 24 h (Table S14 in the Supporting Information) and recrystallized H_2*bpdc* can be observed in the PXRD pattern (Figure S6 in the Supporting Information). The PXRD patterns of the obtained products are similar and reveal the formation of MIL-140C (see Figure 9, right).

Finally, this experiment was repeated with a lower reaction temperature of 120 °C. After 72 h, a crystalline material is obtained, which can be clearly identified as MIL-140C (see Figure 9, left). In the SEM images of the product from the synthesis at 120 °C, the platelet-like morphology of the MIL-140C particles can be seen (Figure S7 in the Supporting Information).

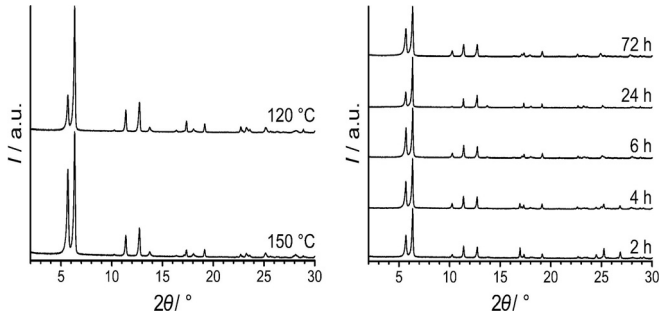

Figure 9. Left: PXRD patterns of MIL-140C syntheses with 80 equivalents of DMF and 30 equivalents of acetic acid at 150 °C and 120 °C after a reaction time of 72 h. Right: PXRD patterns of MIL-140C syntheses with 80 equivalents of DMF and 30 equivalents of acetic acid at 150 °C with increasing reaction time (from bottom to top: 2, 4, 6, 24, and 72 h).

Synthesis of MIL-140D-*sdc*

The published structure of MIL-140D is based on the linker 3,3′-dichloro-4,4′-azobenzenedicarboxylic acid (H_2*abdc*-Cl_2). Owing to the better commercial availability, which makes it easier to conduct systematic investigations, the structurally similar linker molecule 4,4′-stilbenedicarboxylic acid (H_2*sdc*) was used. It shares, in principle, the same structure but its backbone is completely based on carbon atoms and it has no further functional groups at the phenyl rings. Furthermore, the calculated distance (Figure S8 in the Supporting Information) between the carbon atoms of the carboxylate groups of H_2*sdc* (12.4 Å) is slightly larger than that of H_2*abdc*-Cl_2 (12.2 Å). By using H_2*sdc* as the linker under typical MIL-140 synthesis conditions, it was possible for us to prepare a new member of the MIL-140 family, called MIL-140D-*sdc*.

For the description and characterization of this new compound different analyses were carried out. Beside thermogravimetric analysis and sorption measurements (see below), we reproduced the reported MIL-140D with 4,4′-azobenzenedicarboxylic acid as linker (H_2*abdc*) and transferred the reaction conditions to our linker H_2*sdc* with slight adjustments.[20] Furthermore, we developed a structural model for the new MIL-140D-*sdc* for better comparability of the PXRD pattern (see Figure 10 and the Supporting Information). Owing to the longer linker H_2*sdc*, the unit cell parameters of the MIL-140D-*sdc* are slightly larger than those of the previously reported MIL-140D (Table S15 in the Supporting Information).[17] As can be seen, the calculated and experimental patterns of MIL-140D-*sdc* show a very good agreement, especially for the first two diffraction peaks. In comparison to the pattern of the reproduced MIL-140D, the diffraction peaks are slightly shifted to smaller angles.

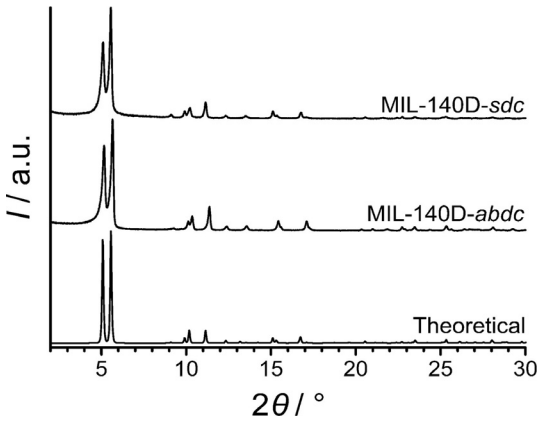

Figure 10. PXRD pattern of the MIL-140D samples synthesized with H_2*abdc*, H_2*sdc*, and the calculated pattern.

Influence of precursor concentration

For the following experiments, the same reaction parameters are chosen as before (150 °C and 24 h reaction time). As already mentioned for the UiO-67 and MIL-140C, a modulator should be essential for MOF syntheses with longer linkers, as it is the case here. The molar ratio of $ZrCl_4$ and H_2*sdc* was kept at 1:1, the amount of DMF was varied between 20 and 120 equivalents, and the amount of acetic acid between 0 and 30 equivalents.

The results of the unmodulated experiments are comparable to those of the experiments for MIL-140C (see Figure 11 a). There is no precipitation of MIL-140D-*sdc*, but with decreasing equivalents of DMF, a sharp reflection appears at approximately $2\theta = 5.30^\circ$. This phase is similar to the product of the MIL-140C synthesis with 20 equivalents of DMF and 0 equivalents of acetic acid but, owing to the longer linker, shifted to smaller angles (see Figure 6 a).

An important factor to be considered is the even poorer solubility of H_2*sdc* in DMF in comparison to H_2*bpdc* and H_2*bdc*. Products form highly concentrated precursor mixtures and show two more reflections (16.46° and 23.43°), which can be assigned to the linker H_2*sdc* (marked in blue).

With a higher amount of acetic acid, the recrystallization of the linker occurs even at higher dilution (see Figure 12). Consequently, the phase-pure synthesis of MIL-140D-*sdc* is also shifted to higher dilutions compared with MIL-140A and MIL-140C (see Figure 11 b–d and Figure S9 in the Supporting Information).

The results of the experiments concerning MIL-140D-*sdc* can be summarized in that either an amorphous phase, the linker, or the MOF precipitates. However, the right precursor concentration seems to be even more important than for MIL-140A and MIL-140C because there are only small variations of the synthesis parameters possible. The linker solubility of H_2*sdc* is even lower than that of H_2*bpdc*. This is the reason why a too concentrated synthesis mixture does not yield the desired product and only the recrystallized linker can be isolated (see Figure 11). The suitable range for the preparation of this material is smaller than for MIL-140C and MIL-140A. Furthermore, for experiments at 150 °C, there is no indication of a product with *fcu* topology like UiO-*sdc*.[29]

Influence of modulator concentration

The systematic investigation of the crystallization behavior of MIL-140D-*sdc* reveals a clear dependency on the precursor

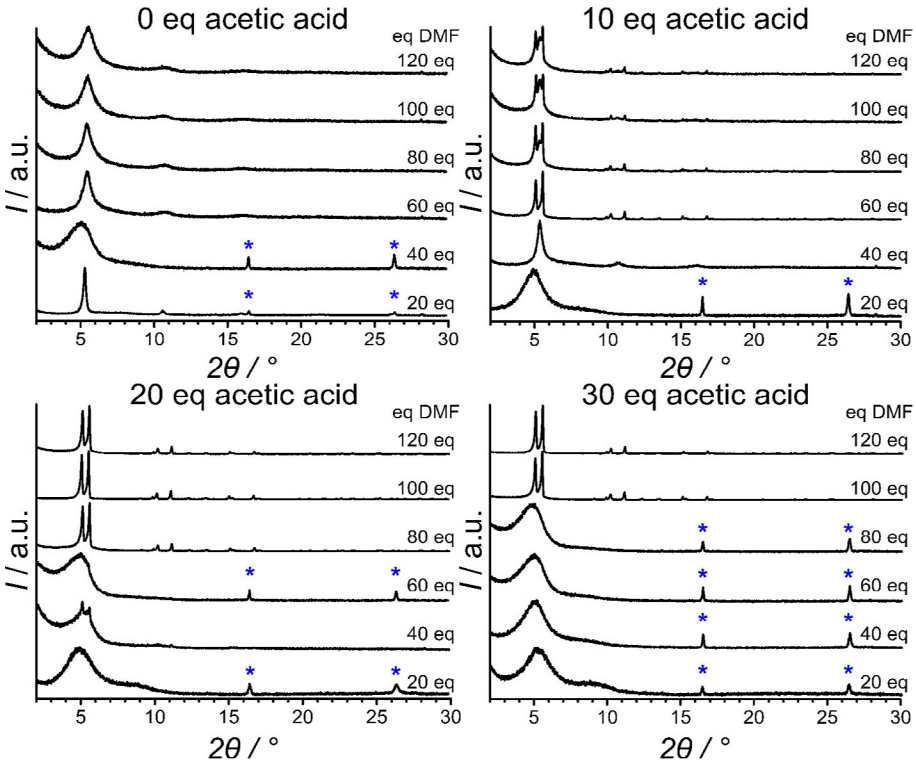

Figure 11. PXRD patterns of the products obtained from the systematic investigation of the formation of MIL-140D-*sdc* with different amounts of acetic acid. The PXRD patterns are arranged according to the amount of DMF from 20 to 120 equivalents. The diffraction peaks of the recrystallized linker H_2*sdc* are marked with blue asterisks.

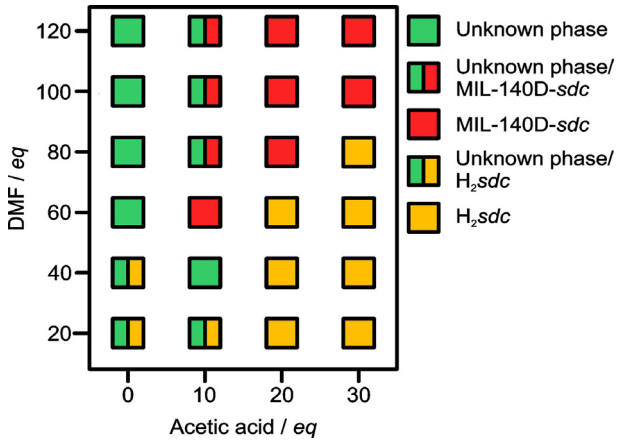

Figure 12. Synthesis field diagram of MIL-140D-*sdc*. The individual phases were assigned from PXRD for products from reactions for 24 h at 150 °C.

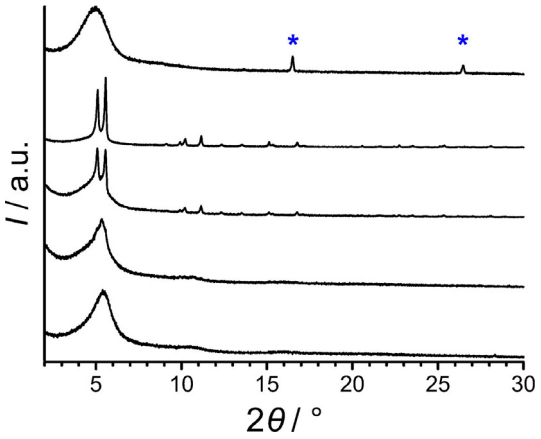

Figure 13. PXRD patterns of the products obtained from a synthesis with an increasing amount of acetic acid (bottom to top: 0, 10, 20, 30, and 40 equiv). The blue marked diffraction peaks can be assigned to the linker H_2*sdc*.

concentration. With an increasing amount of modulator, the solubility of the linker decreases and the area for a successful synthesis is shifted to higher dilution compared with MIL-140A and C. The direct connection between the amount of acetic acid and the formation of MIL-140D-*sdc* can be shown by the results of the following experiments. With a reaction temperature of 150 °C and a reaction time of 72 h, the amount of DMF was set to 120 equivalents and the amount of acetic acid varied between 0 and 40 equivalents.

For the MIL-140D-*sdc*, the presence of a modulator is more crucial than for other MIL-140 MOFs. There is a precipitation of an amorphous product when using a too low amount of modulator and a recrystallization of the linker if the amount is too high (see Figure 13). Only with 20 and 30 equivalents of acetic acid, was a crystalline product obtained but the quality of the PXRD pattern was solely satisfying with 30 equivalents of acetic acid.

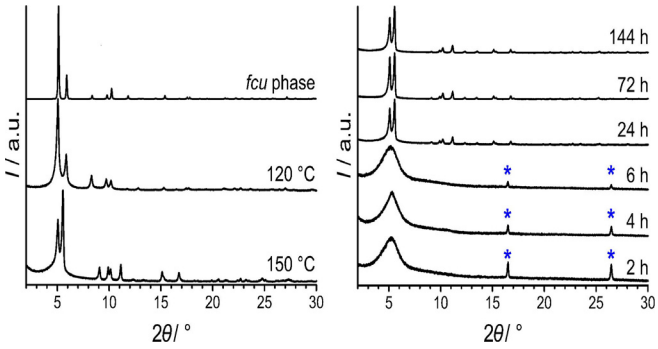

Figure 14. Left: PXRD patterns of MIL-140D-*sdc* syntheses with 120 equivalents DMF and 30 equivalents acetic acid at 150 °C and 120 °C after a reaction time of 72 h in comparison to a calculated pattern of the corresponding phase with *fcu* topology (top).[29] Right: PXRD patterns of MIL-140D-*sdc* syntheses with 120 equivalents DMF and 30 equivalents acetic acid at 150 °C with increasing reaction time (from bottom to top: 2, 4, 6, 24, 72, and 144 h). The diffraction peaks of the recrystallized linker H_2*sdc* are marked with blue asterisks.

Influence of reaction temperature and time

The experiment with 120 equivalents DMF and 30 equivalents acetic acid was repeated with different reaction times and temperatures. In contrast to the MIL-140C, it is not possible to synthesize MIL-140D-*sdc* at 150 °C with short reaction times of less than 6 h (see Figure 14, right). However, with a reaction time of 24 h or more, the diffraction pattern corresponds to the calculated one. Furthermore, there is no indication of the formation of a UiO phase in any experiment. Clearly, the MIL-140 phase is favored over the UiO phase with H_2*sdc* as linker molecule under these conditions.

Finally, the reaction temperature was varied with a constant reaction time of 72 h for the same experiments. In the case of the MIL-140D-*sdc*, this was the first time that formation of the *fcu* phase was observed, with a reaction temperature of 120 °C (see Figure 14, left).[29] Under these conditions, the MIL-140D-*sdc* phase was only obtained with temperatures of 150 °C or higher.

Characterization

In this section, the three MOFs with MIL-140 structure are investigated with physisorption measurements, thermogravimetric analysis, and ^{1}H NMR spectroscopy (reaction parameters in Table S16 in the Supporting Information).

Physisorption measurements with argon at 87 K of Soxhlet-extracted samples (acetone) show an increasing uptake from MIL-140A to MIL-140D-*sdc* (see Figure 15, right). Accordingly, the resulting BET surface is around 280 $m^2 g^{-1}$ for MIL-140A and 730 and 870 $m^2 g^{-1}$ for MIL-140C and MIL-140D-*sdc*. These results are in a very good agreement with the data found in literature (Table S17 in the Supporting Information).[17,20]

With regard to the thermal stability, MIL-140A and MIL-140C show a very similar behavior with a decomposition temperature around 400 to 450 °C in air (see Figure 15, left). MIL-140D-*sdc* exhibits a slightly lower thermal stability of about 300 °C. The experimental weight losses for MIL-140A and MIL-140C correspond well with the calculated values (Table S18 in the Supporting Information). The theoretical and experimental results of MIL-140D-*sdc* exhibit a difference of around 4 *m*% indicating either the formation of ZrO_2 during the synthesis or missing linker molecules in the framework.[30]

To further investigate the composition of the materials and maybe a modulator initiated defect formation, samples of Soxhlet-extracted MIL-140A and MIL-140C were digested in [D_6]DMSO through the addition of HF to evaluate the ratio between linker and modulator molecules. Owing to the low solubility of H_2*sdc* in the [D_6]DMSO/HF mixture, the same procedure for MIL-140D-*sdc* was not possible. The ^{1}H NMR spectra of digested MIL-140A and C reveal that the modulator acetic acid is part of the structure in both materials or at least is so strongly attached to the framework that it cannot be displaced by a Soxhlet extraction with acetone. The molar ratio of acetic acid and linker calculated from the integrals of acetic acid and of the aromatic protons of the linker is 1:9.25 for MIL-140A and 1:13.50 for MIL-140C. This indicates a defect formation during the MOF synthesis by the use of acetic acid (Figure S10 in the Supporting Information) and the low-temperature approach.

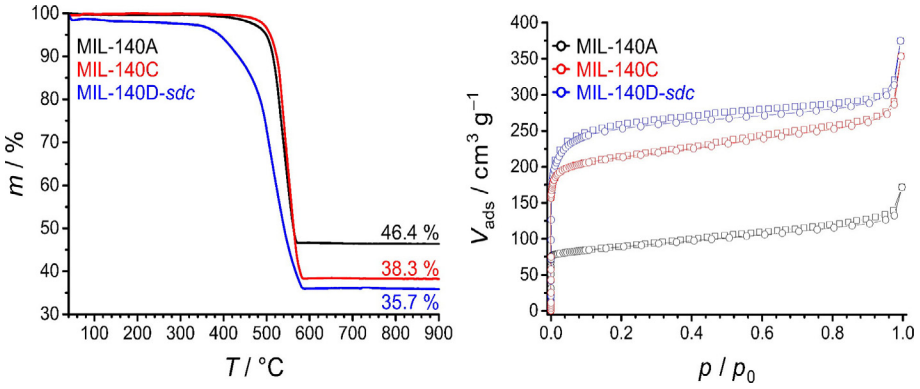

Figure 15. Left: TG analysis of solvent-exchanged (acetone) samples of MIL-140A (black), MIL-140C (red), and MIL-140D-*sdc* (blue) with the experimental residue in percent. Right: Ar physisorption measurements of MIL-140A (black), MIL-140C (red), and MIL-140D-*sdc* (blue) at 87 K. The circles mark the adsorption data and the squares those of the desorption.

The indication of these defects in the MIL-140 MOFs increases the potential to make these class of MOFs even more customizable as is the case for UiO MOFs.[31]

As mentioned above, during the syntheses of MIL-140C and MIL-140D-*sdc* an unknown phase occurs. This phase was further characterized in case of H_2*sdc* as linker molecule. The resulting product shows a BET surface area of 810 $m^2 g^{-1}$ and a high thermal stability of over 450 °C. Both characteristics are comparable to the MIL-140D-*sdc* phase, which enhances the impression of a structurally related phase (Figures S11–S13 in the Supporting Information).

Conclusions

In this work, we focused on the formation of MOFs with MIL-140 structure and presented the synthesis of MIL-140A, MIL-140C, and described MIL-140D-*sdc* for the first time. In contrast to conventional solvothermal MOF syntheses, we used highly concentrated synthesis mixtures with low amounts of DMF in the ranges from 20 to 120 equivalents with respect to $ZrCl_4$ or the linker. We evaluated the crystallization behavior of the three MIL-140 materials yielded from such reaction mixtures. As the thus-obtained synthesis field diagrams reveal, it is possible to control the syntheses to produce phase-pure MIL-140 materials under certain conditions. Keeping other parameters constant, like reaction temperature or the solvent volume, it becomes clear that the outcome of MIL-140 syntheses are highly dependent on the concentration of the precursors, especially of the linker. In other words, a decisive factor is the solubility of the linker in DMF. This can be categorized roughly into three cases. If the linker is completely dissolved in DMF (high amount of DMF, low amount of acetic acid), the corresponding UiO-phase or a phase mixture can be obtained. If the solubility of the linker is very low (low amount of DMF, high amount of acetic acid), a pre-phase or the linker itself is obtained. Only under reaction conditions where the linker is dissolved to some extent and a sufficient amount of solid linker is also present, was a phase-pure MIL-140 phase yielded. From MIL-140A to MIL-140D-*sdc* these zones are shifted to higher dilutions owing to the lower solubility of the used linkers.

The right choice of the synthesis composition enables a further decrease of the reaction temperature for MIL-140A and MIL-140C. We expect that the high precursor concentration promotes the formation of MIL-140 frameworks. Beside the linker solubility, the amount of modulator is also an important parameter for successful synthesis control when the linkers H_2*bpdc* and H_2*sdc* are used.

This work provides valuable synthesis field diagrams, which allow control of the synthesis of MIL-140 materials. The obtained knowledge can be used for a targeted formation of new MOFs with MIL-140 structure with functionalized linkers. Furthermore, with the lower reaction temperature of 120 °C, thermally unstable functional groups can be introduced into the frameworks. This opens the possibility to use these materials for different applications in the future.

Experimental Section

Materials

Zirconium(IV) chloride (> 99.5 %, $ZrCl_4$, Sigma–Aldrich), terephthalic acid (98 %, $C_8H_6O_4$, Sigma–Aldrich), biphenyl-4,4′-dicarboxylic acid (97 %, $C_{14}H_{10}O_4$, Sigma–Aldrich), 4,4′-stilbenedicarboxylic acid (98 %, $C_{16}H_{12}O_4$, ABCR), *N*,*N*-dimethylformamide (99 %, DMF, Sigma–Aldrich), and acetic acid (99 %, CH_3COOH, Sigma–Aldrich) were used as obtained.

MOF synthesis

All MOF syntheses were performed in 100 mL Pyrex glass vessels. As a cleaning step, each vessel was pre-treated with piranha acid to remove potential seeding crystals. In the general synthesis procedure, $ZrCl_4$ (1 equiv) and the linker (1 equiv) were dissolved in a mixture of DMF (5 mL, 20–130 equiv) and acetic acid as modulator (0–5.57 mL, 0–30 equiv). The reaction mixture was heated to temperatures ranging from 120 to 150 °C and for time spans between one and six days. Most of the syntheses were carried out at 150 °C with a reaction time of 24 h. After the vessels were cooled down to room temperature, the resulting product was separated from the liquid phase by centrifugation. The solid was washed once with DMF and acetone. The obtained solids were dried in air at 120 °C overnight. For a more detailed description of the reaction parameters, see the Supporting Information.

Powder X-ray diffraction

PXRD was carried out in transmission mode by using a Stoe Stadi P diffractometer operated with Ge(111)-monochromatized $Cu_{K\alpha1}$ radiation ($\lambda = 1.54060$ Å) and a linear position sensitive detector with scintillation counter.

Thermogravimetric analysis

TGA was performed by using a Netzsch STA 409PC thermoanalyzer. For this purpose, the samples were filled into alumina crucibles and heated under a flow of air at a heating rate of 5 °C min^{-1} up to 1000 °C.

Physisorption measurements

Argon physisorption isotherms were measured at 87 K by using a Quantachrome Autosorb-1 instrument. The samples were solvent-exchanged with acetone by using a Soxhlet extractor and outgassed at 120 °C under vacuum using the Quantachrome Autosorb-1 instrument immediately prior to the measurement.

The "Micropore BET Assistant'' implemented in the ASiQwin 2.0 software from Quantachrome was used to determine the maximum relative pressure for the BET (Brunauer–Emmett–Teller) plot. It determines the BET range according to the theory of Rouquerol, which was shown to be appropriate for the comparison of different MOFs.[32]

Scanning electron microscopy

SEM images were taken with a JSM-6700F field-emission SEM using a beam energy of 2 kV. Samples were dispersed in ethanol and drop-cast on polished graphite supports.

Transmission electron microscopy

For TEM, a FEI Tecnai G2 F20 TMP was used in bright field mode (200 kV). For sample preparation, 400-mesh carbon-coated copper grids (Quantifoil) were used. The samples were dispersed by ultrasonication in ethanol, dropped on the grid, and dried.

^{1}H NMR spectroscopy

For the characterization with ^{1}H NMR spectroscopy, the MOFs (20 mg) were digested in [D_6]DMSO (0.6 mL) through the addition of HF (15 μL, 48 wt%) and stirred for 24 h. Then, $CaCl_2$ was added and the suspension was decanted after a short period of time.

Acknowledgments

General and financial support by Prof. Dr. P. Behrens as well as fruitful discussions are gratefully acknowledged. Another acknowledgement goes to the LNQE (Laboratory of Nano and Quantum Engineering, Leibniz University Hannover) for the opportunity to use their TEM equipment. We thank Hendrik A. Schulze and Thea Heinemeyer for additional SEM images. Open access funding enabled and organized by Projekt DEAL.

Conflict of interest

The authors declare no conflict of interest.

Keywords: hybrid materials · metal–organic frameworks · MIL-140 · phase purity · synthesis field diagrams

[1] S. Kitagawa, R. Kitaura, S.-i. Noro, *Angew. Chem. Int. Ed.* **2004**, *43*, 2334 – 2375; *Angew. Chem.* **2004**, *116*, 2388 – 2430.
[2] O. K. Farha, I. Eryazici, N. C. Jeong, B. G. Hauser, C. E. Wilmer, A. A. Sarjeant, R. Q. Snurr, S. T. Nguyen, A. Ö. Yazaydın, J. T. Hupp, *J. Am. Chem. Soc.* **2012**, *134*, 15016 – 15021.
[3] C. Janiak, J. K. Vieth, *New J. Chem.* **2010**, *34*, 2366 – 2388.
[4] M. Kim, S. M. Cohen, *CrystEngComm* **2012**, *14*, 4096 – 4104.
[5] H. Bux, A. Feldhoff, J. Cravillon, M. Wiebcke, Y.-S. Li, J. Caro, *Chem. Mater.* **2011**, *23*, 2262 – 2269.
[6] D. Cunha, C. Gaudin, I. Colinet, P. Horcajada, G. Maurin, C. Serre, *J. Mater. Chem. B* **2013**, *1*, 1101 – 1108.
[7] F. Vermoortele, B. Bueken, G. Le Bars, B. van de Voorde, M. Vandichel, K. Houthoofd, A. Vimont, M. Daturi, M. Waroquier, V. van Speybroeck, C. Kirschhock, D. E. de Vos, *J. Am. Chem. Soc.* **2013**, *135*, 11465 – 11468.
[8] a) L. E. Kreno, K. Leong, O. K. Farha, M. Allendorf, R. P. van Duyne, J. T. Hupp, *Chem. Rev.* **2012**, *112*, 1105 – 1125; b) M. Schulz, A. Gehl, J. Schlenkrich, H. A. Schulze, S. Zimmermann, A. Schaate, *Angew. Chem. Int. Ed.* **2018**, *57*, 12961 – 12965; *Angew. Chem.* **2018**, *130*, 13143 – 13147.
[9] J. H. Cavka, S. Jakobsen, U. Olsbye, N. Guillou, C. Lamberti, S. Bordiga, K. P. Lillerud, *J. Am. Chem. Soc.* **2008**, *130*, 13850 – 13851.
[10] J. J. Low, A. I. Benin, P. Jakubczak, J. F. Abrahamian, S. A. Faheem, R. R. Willis, *J. Am. Chem. Soc.* **2009**, *131*, 15834 – 15842.
[11] J. B. DeCoste, G. W. Peterson, H. Jasuja, T. G. Glover, Y.-g. Huang, K. S. Walton, *J. Mater. Chem. A* **2013**, *1*, 5642 – 5650.
[12] A. Schaate, P. Roy, A. Godt, J. Lippke, F. Waltz, M. Wiebcke, P. Behrens, *Chem. Eur. J.* **2011**, *17*, 6643 – 6651.
[13] a) J. E. Mondloch, M. J. Katz, N. Planas, D. Semrouni, L. Gagliardi, J. T. Hupp, O. K. Farha, *Chem. Commun.* **2014**, *50*, 8944 – 8946; b) N. Ko, J. Hong, S. Sung, K. E. Cordova, H. J. Park, J. K. Yang, J. Kim, *Dalton Trans.* **2015**, *44*, 2047 – 2051.
[14] a) S. Biswas, P. van der Voort, *Eur. J. Inorg. Chem.* **2013**, 2154 – 2160; b) M. J. Katz, Z. J. Brown, Y. J. Colón, P. W. Siu, K. A. Scheidt, R. Q. Snurr, J. T. Hupp, O. K. Farha, *Chem. Commun.* **2013**, *49*, 9449 – 9451.
[15] G. E. Cmarik, M. Kim, S. M. Cohen, K. S. Walton, *Langmuir* **2012**, *28*, 15606 – 15613.
[16] M. Kim, J. F. Cahill, H. Fei, K. A. Prather, S. M. Cohen, *J. Am. Chem. Soc.* **2012**, *134*, 18082 – 18088.
[17] V. Guillerm, F. Ragon, M. Dan-Hardi, T. Devic, M. Vishnuvarthan, B. Campo, A. Vimont, G. Clet, Q. Yang, G. Maurin, G. Férey, A. Vittadini, S. Gross, C. Serre, *Angew. Chem. Int. Ed.* **2012**, *51*, 9267 – 9271; *Angew. Chem.* **2012**, *124*, 9401 – 9405.
[18] K. Dedecker, R. S. Pillai, F. Nouar, J. Pires, N. Steunou, E. Dumas, G. Maurin, C. Serre, M. L. Pinto, *ACS Appl. Mater. Interfaces* **2018**, *10*, 13886 – 13894.
[19] R. D'Amato, A. Donnadio, M. Carta, C. Sangregorio, D. Tiana, R. Vivani, M. Taddei, F. Costantino, *ACS Sustainable Chem. Eng.* **2019**, *7*, 394 – 402.
[20] W. Liang, R. Babarao, T. L. Church, D. M. D'Alessandro, *Chem. Commun.* **2015**, *51*, 11286 – 11289.
[21] W. Liang, R. Babarao, D. M. D'Alessandro, *Inorg. Chem.* **2013**, *52*, 12878 – 12880.
[22] W. Liang, D. M. D'Alessandro, *Chem. Commun.* **2013**, *49*, 3706 – 3708.
[23] V. V. Butova, A. P. Budnyk, K. M. Charykov, K. S. Vetlitsyna-Novikova, C. Lamberti, A. V. Soldatov, *Chem. Commun.* **2019**, *55*, 901 – 904.
[24] S. Wang, Y. Liao, O. K. Farha, H. Xing, C. A. Mirkin, *Chem. Mater.* **2018**, *30*, 4877 – 4881.
[25] H. A. Henthorn, M. D. Pluth, *J. Am. Chem. Soc.* **2015**, *137*, 15330 – 15336.
[26] a) T. C. Wang, W. Bury, D. A. Gómez-Gualdrón, N. A. Vermeulen, J. E. Mondloch, P. Deria, K. Zhang, P. Z. Moghadam, A. A. Sarjeant, R. Q. Snurr, J. F. Stoddart, J. T. Hupp, O. K. Farha, *J. Am. Chem. Soc.* **2015**, *137*, 3585 – 3591; b) G. Wißmann, A. Schaate, S. Lilienthal, I. Bremer, A. M. Schneider, P. Behrens, *Microporous Mesoporous Mater.* **2012**, *152*, 64 – 70.
[27] W. Morris, W. E. Briley, E. Auyeung, M. D. Cabezas, C. A. Mirkin, *J. Am. Chem. Soc.* **2014**, *136*, 7261 – 7264.
[28] B. van de Voorde, D. Damasceno Borges, F. Vermoortele, R. Wouters, B. Bozbiyik, J. Denayer, F. Taulelle, C. Martineau, C. Serre, G. Maurin, D. de Vos, *ChemSusChem* **2015**, *8*, 3159 – 3166.
[29] R. J. Marshall, T. Richards, C. L. Hobday, C. F. Murphie, C. Wilson, S. A. Moggach, T. D. Bennett, R. S. Forgan, *Dalton Trans.* **2016**, *45*, 4132 – 4135.
[30] a) G. C. Shearer, S. Chavan, S. Bordiga, S. Svelle, U. Olsbye, K. P. Lillerud, *Chem. Mater.* **2016**, *28*, 3749 – 3761; b) G. C. Shearer, S. Chavan, J. Ethiraj, J. G. Vitillo, S. Svelle, U. Olsbye, C. Lamberti, S. Bordiga, K. P. Lillerud, *Chem. Mater.* **2014**, *26*, 4068 – 4071; c) R. J. Marshall, C. L. Hobday, C. F. Murphie, S. L. Griffin, C. A. Morrison, S. A. Moggach, R. S. Forgan, *J. Mater. Chem. A* **2016**, *4*, 6955 – 6963.
[31] G. C. Shearer, J. G. Vitillo, S. Bordiga, S. Svelle, U. Olsbye, K. P. Lillerud, *Chem. Mater.* **2016**, *28*, 7190 – 7193.
[32] a) Y.-S. Bae, A. O. Yazaydin, R. Q. Snurr, *Langmuir* **2010**, *26*, 5475 – 5483; b) K. S. Walton, R. Q. Snurr, *J. Am. Chem. Soc.* **2007**, *129*, 8552 – 8556.

Manuscript received: June 28, 2019
Revised manuscript received: July 29, 2019
Accepted manuscript online: August 9, 2019
Version of record online: September 18, 2019

